

Origin of visible luminescence in hydrogenated amorphous silicon nitride

H. L. Hao, L. K. Wu, and W. Z. Shen^{a)}

Laboratory of Condensed Matter Spectroscopy and Opto-Electronic Physics, Department of Physics, Shanghai Jiao Tong University, 1954 Hua Shan Road, Shanghai 200030, People's Republic of China

H. F. W. Dekkers

Solar Cell Technology, IMEC vzw, Kapeldreef 75, B-3001 Leuven, Belgium

(Received 28 August 2007; accepted 29 October 2007; published online 16 November 2007)

We present a detailed investigation on the origin of the room-temperature visible luminescence in hydrogenated amorphous silicon nitride films. In combination with Raman spectroscopy and high resolution transmission electron microscopy, we demonstrate clearly that the red light emission originates from amorphous silicon quantum dots. On the basis of the redshift of peak position, narrowing of bandwidth, and temperature quenching of luminescence, we attribute the green emission to the bandtail recombination of carriers. In addition, the blue luminescence is assigned to the silicon-related defects according to the analysis for the gap states in silicon nitride. © 2007 American Institute of Physics. [DOI: 10.1063/1.2814053]

Over a decade, the observation of strong room-temperature visible luminescence from porous silicon has attracted researchers to explore silicon-based materials for their potential applications in light-emitting devices (LEDs). The previous interest was on the light emission from silicon nanostructures in silicon oxide films. However, theoretical and experimental investigations suggest that there are extremely high potential barriers (~ 8.5 eV) for silicon oxide with silicon nanocrystals,¹ which seriously decrease the injection efficiency of carriers. Recently, enormous attention has been paid to the light emission from silicon nitride films with silicon quantum dots (Si QDs), which show relatively lower barrier (~ 2.0 eV) for carriers and more intense light emission than those of silicon oxide.²⁻⁵ Thus, silicon nitride films embedded with Si QDs represent good candidates for the silicon-based LEDs.

Considerable visible photoluminescence (PL) spectra of silicon nitride films have been investigated, and several kinds of radiative recombination centers have been proposed in the nonstoichiometric silicon nitride films.^{6,7} However, the origin of the visible luminescence is still controversial, primarily due to a lack of distinction between luminescence originating from silicon nanoclusters and from silicon nitride matrix. Some assign the luminescence to the quantum confinement effect of silicon nanoclusters in silicon-rich silicon nitride films,^{4,8} while others attribute it to radiative defects recombination or to electron-phonon coupling, and so on.^{6,9} It is significant to clarify the detailed luminescence mechanisms to meet the expectation of the silicon-based LEDs in different visible light ranges.

The studied hydrogenated amorphous silicon nitride (α -SiN_x:H) films (with thickness of ~ 350 – 380 nm) were deposited using a low frequency (440 kHz) plasma enhanced chemical vapor deposition (PECVD) system on ~ 0.5 mm thick *p*-type crystalline silicon substrates. Our recent study demonstrates the great importance of the deposition temperature (T_d) on the microstructure of silicon nitride films.¹⁰ Samples were named by S_x ($x=1, 2, 3, 4$) for T_d at 200, 300, 400, and 500 °C, respectively. Precursor gases were NH₃

and SiH₄ with a constant NH₃:SiH₄ flux ratio of 1700:455. PL and Raman scattering spectra were performed on a Jobin Yvon LabRAM HR 800 UV micro-Raman spectrometer using 325 nm line of He–Cd laser. Infrared absorption spectra were measured at a Nicolet Nexus 870 Fourier transform infrared spectrometer from 400 to 4000 cm⁻¹, subtracted from the substrate absorption contribution. The ultraviolet reflection measurements were carried out in the range of 3.1–4.7 eV using a Jobin Yvon 460 monochromator. All the optical spectra were recorded at room temperature.

Figure 1(a) shows PL spectra of the samples. We have decomposed the PL spectra into three Gaussian peaks, and these PL bands present different characteristics under different T_d . In the near-infrared to red light range, the Gaussian peak in S1 is almost negligible, while those of S2–S4 exhibit an obvious redshift from 1.91 eV in S2 to 1.74 eV in S4. The green PL peak shifts continuously toward the low energy side from 2.40 to 2.05 eV in S1–S4. However, the blue PL peak energy keeps almost unchanged in these samples. It is reasonable to assume that there are different emission mechanisms responsible for these luminescence peaks.

We begin with the investigation of the luminescence mechanism for the PL band in the near-infrared to red light range. Figure 2 displays the Raman spectra of the samples. Longitudinal optical band centers at around 385 cm⁻¹. Trans-

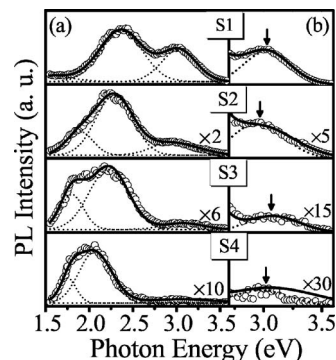


FIG. 1. (a) PL spectra (open circles) of α -SiN_x:H films under excitation of 325 nm, the solid curves are the overall fitting results using three Gaussian peaks (dotted curves). (b) The magnified blue bands with the arrows to the PL peaks.

^{a)} Author to whom correspondence should be addressed. Electronic mail: wzshen@sjtu.edu.cn

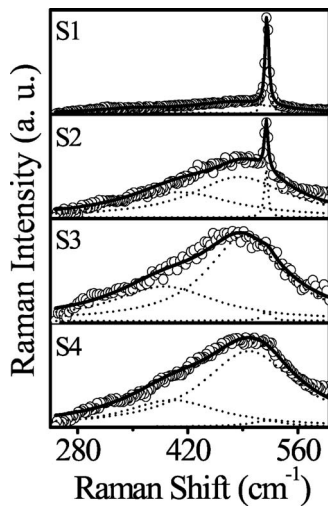


FIG. 2. Experimental (open circles) and calculated (solid curves) Raman spectra with three Lorentz phonon bands (dotted curves).

verse optical (TO_1) band is in the range from 480 to 498 cm^{-1} , where the typical Raman spectra of amorphous silicon quantum dots (α -Si QDs) lie.¹¹ The narrow TO band at about 520 cm^{-1} comes from the monocrystalline silicon substrates.¹² Due to the higher NSi ratio [1.09, from Rutherford backscattering spectroscopy (RBS) measurements] at $T_d=200$ °C, TO_1 signal in S1 is very weak, indicating that there are very few Si QDs in S1.² With the increase of T_d , the NSi ratio decreases from 1.00 in S2 to 0.97 in S4, TO_1 shifts from 492 to 498 cm^{-1} , suggesting the increase of the Si QDs size.¹³ According to the calculation of the Raman shift confinement model,¹⁴ the size of Si QD has an increment of about 1.7 nm for the increasing Raman shift of 6 cm^{-1} . The Raman results indicate that the negligible PL peak of S1 is due to the very few α -Si QDs in the silicon nitride matrix, which is consistent with the observation in Ref. 13, while the redshift of the luminescence peak in S2–S4 is associated with the increase of α -Si QDs size as a result of the quantum confinement effect (QCE).^{4,15}

The existence and evolution of α -Si QDs in silicon nitride films can be directly confirmed by the high resolution transmission electron microscopy (HRTEM) and infrared absorption measurements. Figure 3(a) presents the cross-sectional HRTEM image of S2, where the α -Si QDs with higher density than the silicon nitride matrix appear as dark spots. The average dot size is about 3.1 nm, which is in good agreement with the size of ~ 3.0 nm for the red emission according to the QCE model for α -Si QDs.⁴ The transmission electron diffraction pattern in Fig. 3(b) shows a bright single diffuse ring, further verifying that the Si QDs are amorphous; this is due to the high growth rate during the deposition process (>4 nm/min).¹⁶

Figure 3(c) shows the infrared absorption spectrum of S2. The absorption bands at 610, 830, 1100, 2170, and 3330 cm^{-1} can be assigned to the modes of Si-H bending, Si-N stretching, N-H rocking, Si-H stretching, and N-H stretching, respectively. The densities of the Si-H, Si-N, and N-H bonds have been calculated [shown by Fig. 3(d)] via the formula $K \int \alpha(\omega) \omega d\omega$, where K is the calibration factor of these bonds,¹⁷ ω is wave number, and $\alpha(\omega)$ is the absorption coefficient. It is clear that with increase of T_d , the densities of Si-H and N-H bonds decrease, while those of Si-N

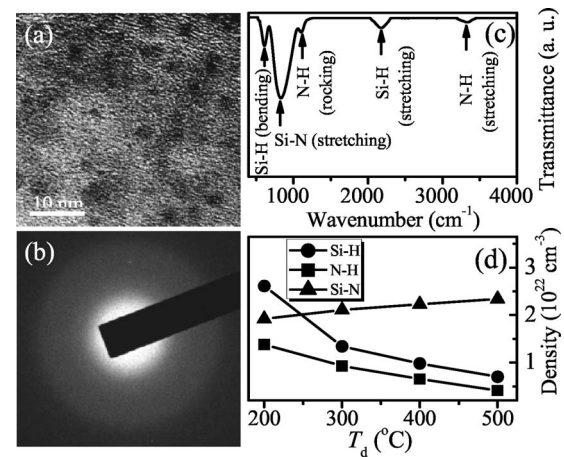


FIG. 3. (a) Cross-sectional HRTEM image of S2, (b) ring pattern for the transmission electron diffraction from α -Si QDs. (c) Infrared absorption spectrum for S2, and (d) densities of SiH, NH, and SiN bonds as a function of deposition temperature T_d .

bonds increase. As we know, the Si-H bonds can be broken to provide the silicon nucleus for the formation of the α -Si QDs. The low T_d in S1 will yield the very low distribution density of α -Si QDs. Under higher T_d , more NH_3 effuse from the silicon nitride top layer during deposition,¹⁸ and the Si-H bonds are easier to be broken, leading to a higher silicon concentration in the film. However, the α -Si QDs formed will congregate and grow up with further increase of T_d above 300 °C, resulting in the formation of large-size α -Si QDs. It should be noted that with the increase of T_d , the hydrogen-related bonds decrease due to more NH_3 effusing, and could not passivate well the nonradiative defects existing at the interface between Si QDs and the silicon nitride matrix, thus leading to the decrease of PL intensity in S2–S4 [see Fig. 1(a)].

We now focus on the effect of T_d on the green PL. With the increase of T_d , the green PL peak shifts toward the low energy side, and the fitted full width at half maximum (FWHM) decreases from 0.51 to 0.30 eV simultaneously [see Fig. 1(a)]. These features are similar to those of PL bands reported in α -SiN_x and amorphous silicon carbon, which is considered to arise from bandtail radiative recombination. Further evidence of that assignment comes from the reflection measurements. Figure 4(a) shows the experimental

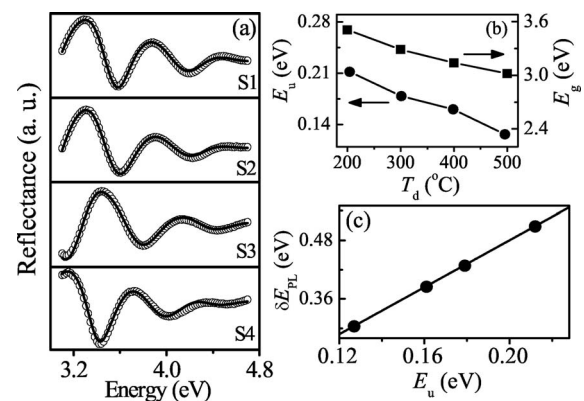


FIG. 4. (a) Experimental (open circles) and theoretical (solid curves) ultraviolet reflectance spectra of α -SiN_x:H. (b) Optical band gap E_g and Urbach tail E_U of α -SiN_x:H films vs T_d , and (c) relationship between E_U and FWHM of green PL δE_{PL} .

(open circles) and well fitted (solid curves) ultraviolet reflection spectra of the samples, based on the Tauc-Lorentz-Urbach (TLU) model.¹⁰ The yielded optical band gap (E_g) and Urbach tail (E_U) from the TLU fitting as a function of T_d are displayed in Fig. 4(b). With increasing T_d , E_g decreases due to the decrease of NSi ratio, therefore, leading to the significant redshift of the green PL peak.¹⁹ On the other hand, E_U decreases monotonically with the enhancement of T_d , suggesting that narrower bandtail and more ordered silicon nitride network can be achieved at higher T_d .

To study the broadening mechanism of the green PL band, we have examined the relationship between the FWHM and E_U . The closed circles in Fig. 4(c) represent the yielded values from the Gaussian and TLU fittings, and the straight line is the calculated results through the static disorder model:²⁰ $(\delta E_{\text{PL}})^2 = (\xi E_U)^2 + (\delta E_{\text{e-ph}})^2$, with δE_{PL} the FWHM of the PL spectra, ξ a coefficient, and $\delta E_{\text{e-ph}}$ the coupling term between electron and phonon. We can see that $\delta E_{\text{e-ph}}$ increases linearly with E_U , and the intercept $\delta E_{\text{e-ph}}$ is about 0.001 eV, much less than the typical phonon energy of 0.060 eV.¹⁹ This strongly indicates that the electron-phonon coupling can be neglected, and the FWHM of the green PL band depends positively on the width of bandtail.

Further insight into the green luminescence mechanism can be achieved by the temperature dependence of PL measurements. The observed quenching of the green luminescence in 83–303 K for all these samples is the characteristic of the bandtail radiative recombination in SiN_x .²¹ The temperature quenching of the luminescence intensity is found to be enhanced at high T_d , with the activation energy increasing from 86.8 meV in S1 to 100.6 meV in S4. This result reveals that the activation barrier surrounding the recombination centers is larger at higher T_d , and the diffusion and radiative recombination rates of the carriers captured in localized states are reduced.²² Furthermore, narrower bandtail (smaller E_U) at higher T_d would increase thermal excitation of carriers from tail states to extended states, through which carriers recombine via nonradiative processes.¹⁹

Finally, we discuss the origin of the blue luminescence band. It is seen from Fig. 1(b) that the blue band lies in the small range of 3.00 ± 0.05 eV with a negligible variation of FWHM (0.45 ± 0.05 eV), and can be considered almost unchanged with T_d . Theoretical model has predicted that the peak position of defect-related PL depends only on the defect energy level, it is almost fixed for a given defect, and will not be easily controlled.¹⁵ Several works have demonstrated that the 3.0 ± 0.1 eV peak originates from defect-related states in $\alpha\text{-SiN}_x$ PL spectra,^{6,13} and attributed it to the recombination either from the conduction band to the N_2^0 level or from the valence band to the N_4^+ level. However, high annealing temperature (>500 °C) is usually required to generate these nitrogen defects in silicon nitride.²³ Our films are as-deposited without any postannealing treatment, so nitrogen defects would not be created, thus excluding the possibility of nitrogen defects for the blue PL band.

According to Robertson's theoretical calculation through tight-binding method for gap states in $\alpha\text{-SiN}_x$,²⁴ the states of $\equiv\text{Si}^0$ and $\equiv\text{Si}\equiv\text{Si}$ lie about 3.1 and 0.1 eV above the valence band, respectively, the radiative recombination between the two states can generate the PL peak at ~ 3.0 eV. Further evidence of that assignment comes from the dependence of the defect-related PL intensity on T_d . On one hand,

with the increase of T_d , the $\equiv\text{Si}^0$ dangling bonds and $\equiv\text{Si}-\text{Si}\equiv$ units would decrease due to the increase of the Si-N bonds induced by the severe nitridation process.²⁵ On the other hand, higher T_d will hinder the diffusion of hydrogen, which decreases significantly the randomness of the $\alpha\text{-SiN}_x\text{:H}$ network, resulting in fewer silicon defects. As a result of the reduction of silicon defect density, the blue PL intensity is expected to decrease significantly with increasing T_d , as clearly observed in Fig. 1(b). Therefore, the blue emission can be attributed to the electronic transitions of $\equiv\text{Si}^0 \rightarrow \equiv\text{Si}-\text{Si}\equiv$,²⁶ the presence of silicon dangling bond defects has been confirmed by spin resonance measurements.²⁷

This work was supported by the Natural Science Foundation of China (Contract Nos. 10674094 and 10734020), National Major Basic Research Project of 2006CB921507, the Minister of Education of PCSIRT of IRT0524, and the Shanghai Project of 06JC14039. Thanks is due to V. Verlaan at the Utrecht University for RBS measurements.

¹Y. Q. Wang, Y. G. Wang, L. Cao, and Z. X. Cao, Appl. Phys. Lett. **83**, 3474 (2003).

²V. A. Volodin, M. D. Efremov, V. A. Gritsenko, and S. A. Kochubei, Appl. Phys. Lett. **73**, 1212 (1998).

³N.-M. Park, T.-S. Kim, and S.-J. Park, Appl. Phys. Lett. **78**, 2575 (2001).

⁴N.-M. Park, C.-J. Choi, T.-Y. Seong, and S.-J. Park, Phys. Rev. Lett. **86**, 1355 (2001).

⁵K. S. Cho, N.-M. Park, T.-Y. Kim, K.-H. Kim, and G. Y. Sung, Appl. Phys. Lett. **86**, 071909 (2005).

⁶S. V. Deshpande, E. Gulari, S. W. Brown, and S. C. Rand, J. Appl. Phys. **77**, 6534 (1995).

⁷H. Kato, N. Kashio, Y. Ohki, K. S. Seol, and T. Noma, J. Appl. Phys. **93**, 239 (2003).

⁸T.-W. Kim, C.-H. Cho, B.-H. Kim, and S.-J. Park, Appl. Phys. Lett. **88**, 123102 (2006).

⁹K. Yamaguchi, K. Mizushima, and K. Sassa, Appl. Phys. Lett. **77**, 3773 (2000).

¹⁰J. J. Mei, H. Chen, W. Z. Shen, and H. F. W. Dekkers, J. Appl. Phys. **100**, 073516 (2006).

¹¹M. Xu, S. Xu, J. W. Chai, J. D. Long, and Y. C. Ee, Appl. Phys. Lett. **89**, 251904 (2006).

¹²H. Chen, W. Z. Shen, and W. S. Wei, Appl. Phys. Lett. **88**, 121921 (2006).

¹³M. H. Wang, D. S. Li, Z. Z. Yuan, D. R. Yang, and D. L. Que, Appl. Phys. Lett. **90**, 131903 (2007).

¹⁴J. Zi, H. Büscher, C. Falter, W. Ludwig, K. Zhang, and X. Xie, Appl. Phys. Lett. **69**, 200 (1996).

¹⁵B.-H. Kim, C.-H. Cho, T.-W. Kim, N.-M. Park, G. Y. Sung, and S.-J. Park, Appl. Phys. Lett. **86**, 091908 (2005).

¹⁶T.-Y. Kim, N.-M. Park, K.-H. Kim, G.-Y. Sung, Y.-W. Ok, T.-Y. Seong, and C.-J. Choi, Appl. Phys. Lett. **85**, 5355 (2004).

¹⁷S. Hasegawa, L. He, Y. Amano, and T. Inokuma, Phys. Rev. B **48**, 5315 (1993).

¹⁸D. L. Smith, A. S. Alimonda, C.-C. Chen, S. E. Ready, and B. Wacker, J. Electrochem. Soc. **137**, 614 (1990).

¹⁹F. Giorgis, C. Vinegoni, and L. Pavesi, Phys. Rev. B **61**, 4693 (2000).

²⁰T. M. Searle and W. A. Jackson, Philos. Mag. B **60**, 237 (1989).

²¹G. Z. Yue, J. D. Lorentzen, J. Lin, D. X. Han, and Q. Wang, Appl. Phys. Lett. **75**, 492 (1999).

²²L. Dal Negro, J. H. Yi, J. Michel, L. C. Kimerling, T.-W. F. Chang, V. Sukhovatkin, and E. H. Sargent, Appl. Phys. Lett. **88**, 233109 (2006).

²³R. Huang, K. Chen, B. Qian, S. Chen, W. Li, J. Xu, Z. Y. Ma, and X. F. Huang, Appl. Phys. Lett. **89**, 221120 (2006).

²⁴J. Robertson and M. J. Powell, Appl. Phys. Lett. **44**, 415 (1984).

²⁵Z. Lu, P. Santos-Filho, G. Stevens, M. J. Williams, and G. Lucovsky, J. Vac. Sci. Technol. A **13**, 607 (1995).

²⁶C. M. Mo, L. D. Zhang, L. Y. Xie, and T. Wang, J. Appl. Phys. **73**, 5185 (1993).

²⁷W. L. Warren, P. M. Lenahan, and S. E. Carry, Phys. Rev. Lett. **65**, 207 (1991).